Analysis of thermal stratification phenomena in the CIRCE-HERO Facility

F. Buzzi, A. Pucciarelli, F. Galleni, M. Tarantino, N. Forgione

Pre Print

Abstract

In the present paper, CFD simulations related to the operating conditions considered during the experimental campaign on CIRCE-HERO facility, a LBE large pool recently run at ENEA Brasimone RC, are presented. The main purpose is to investigate the temperature stratification phenomena observed inside the CIRCE pool. Calculations are performed using the commercial codes STAR-CCM+ and ANSYS Fluent adopting a RANS approach; the numerical results and the experimental data are compared. Four distinct experimental tests with different boundary conditions are investigated. For each test, several simulations were performed in order to understand the influence of assumptions made regarding the boundary conditions. In particular, assumptions concerning the heat losses distribution and the simplified geometrical shape of some of the relevant thermal structures were taken into account.

The obtained results provide support for further understanding of the involved phenomena, suggesting the possible causes of the thermal stratification observed experimentally inside the pool.

1. Introduction

The analysis of thermal-hydraulics of liquid metals is a relevant issue in the development of Gen. IV nuclear power plants. Liquid metals have interesting capabilities both in terms of nuclear characteristics, allowing a fast neutrons spectrum, and in terms of safety. In fact, the very high boiling temperature assures the core to be constantly wetted practically excluding the risk of dry-out. In addition, being dense fluids, they allow adopting natural convection as a valid mechanism for reactor cooling in both design and accidental conditions. As a consequence, the analysis and comprehension of convection heat transfer mechanism in liquid metals are of fundamental relevance. During the last few years, several experimental facilities have been designed (e.g. NACIE-UP, Di Piazza et al., 2013; CIRCE-ICE, Tarantino et al., 2011; CIRCE-HERO, Pesetti et al., 2018a) for the investigation of thermal-hydraulics in liquid metals, chiefly LBE, allowing the analysis of both natural and forced convection conditions. Due to the intrinsic difficulties in the measurement operations when dealing with liquid metals (e.g. due to solidification issues, fluid storage, oxidation), a strong cooperation between experimentalists and the researchers performing numerical simulations is required in order to better understand the involved phenomena.

In this sense, during the last years the University of Pisa has carried on a productive partnership with the ENEA Brasimone RC, providing numerical support for several experimental campaigns involving liquid metals (Martelli et al., 2014, Narcisi et al., 2017, Martelli et al., 2017a). In the present paper, the CIRCE-HERO facility (Pesetti et al., 2018a) is in particular considered. The facility has been designed in order to investigate forced and natural circulation phenomena in pool-type LMFBRs and proved to be an interesting workbench for assessing the capabilities of CFD and STH codes, both running in stand-alone or coupled applications. At the University of Pisa, several studies have been performed both focusing on single components (Martelli et al., 2017b) or on the whole facility (Gonfiotti et al., 2018). In the present paper only the pool is considered, mainly focusing on the heat transfer phenomena between the primary system components and the fluid at rest or in natural circulation in the pool. Recent experiments reported the occurrence of thermal stratification phenomena inside the pool (Lorusso et al., 2018). The present paper tries to reproduce such behaviours by performing CFD analyses adopting the commercial codes STAR-CCM+ (Siemens, 2019) and ANSYS Fluent (2019). In comparison to previous studies performed at the University of Pisa (Angelucci et al., 2017b), a more refined mesh is adopted in order to take into account the small buoyancy phenomena which may occur in the vicinity of the heated walls and allowing a better analysis of the heat losses towards the environment. The obtained results are promising and provide interesting information for the comprehension of the thermal-hydraulics aspects of the CIRCE pool, suggesting possible strategies for the simulation of the whole facility. In this sense, this work represents a further step in the development of coupled STH/CFD applications which are currently being carried on at the University of Pisa (Angelucci et al., 2017a; Martelli et al., 2017; Forgione et al., 2019). A better characterization of the pool thermal-hydraulics and the assessment of the CFD

Pre Print

capabilities in reproducing the observed phenomena is in fact of capital importance for the success of these applications.

2. Experimental facility

CIRCulation Eutectic (CIRCE) is a multipurpose cylindrical pool type facility and it is designed with the aim of supporting the development of heavy liquid metal pool-type reactor.

The CIRCE facility consists in a 1200 mm diameter and 8500 mm height vessel filled with about 70 tonnes of molten Lead-Bismuth Eutectic (LBE); argon is used as cover gas in order to prevent contact between LBE and air. The Heavy liquid mEtal-pRessurised water cOoled tube (HERO) heat exchanger is located inside the CIRCE pool as a main component of the test section. Other relevant components are: the Fuel Pin Simulator (FPS), which represents the facility heat source, composed by 37 pins arranged inside a hexagonal wrapper; a Fitting Volume (FV), a Riser, a Separator (SP). HERO Steam Generator Bayonet Tube (SGBT) represents the cold heat sink. Figure 1 reports a sketch of the facility, also highlighting the most relevant components. This design allows natural circulation inside the test section; circulation can be also enhanced thanks to the injection of argon at the basis of the Riser component. The Riser and the HERO-SGBT were designed to be insulated from the pool. The HERO-SGBT consists in fact of a hexagonal wrap containing 7 circular bayonet tubes in which steam flows; an external cylindrical shroud concentric to the hexagon generates a meatus filled by air which provides thermal insulation. Heat transfer is instead possible for all the other components. The CIRCE vessel is insulated as well; however, as demonstrated during the experimental tests, heat losses towards the environment cannot be considered negligible (Pesetti et al., 2018b).

Axial temperature measurements in the pool were obtained using 122 thermocouples located in different azimuthal positions (see Figure 2) and heights; mass flow is instead measured through a Venturi flow meter positioned at the inlet of the FPS.

Recently, at the ENEA research center in Brasimone, an experimental campaign aiming at investigating the thermal stratification phenomena occurring in the CIRCE pool was carried out (Lorusso et al., 2018). Four experimental cases were selected and analysed in the present work, which are considered representative of the whole addressed data set. Table *1* reports the presently considered experimental conditions.

	Mass Flow rate [kg/s]	FPS Thermal Power [kW]	Inlet Temperature [°C]	FPS bottom Temperature [°C]	FV Temperature [°C]	SP Temperature [°C]
Test Reference	30	90	222	221	240	237
Test 1	31	140	232	231	263	258
Test 2	29	27	209	207	214	213
Test 3	39	90	223	222	237	235

Pre Print

Table 1: Operating conditions considered in the present paper

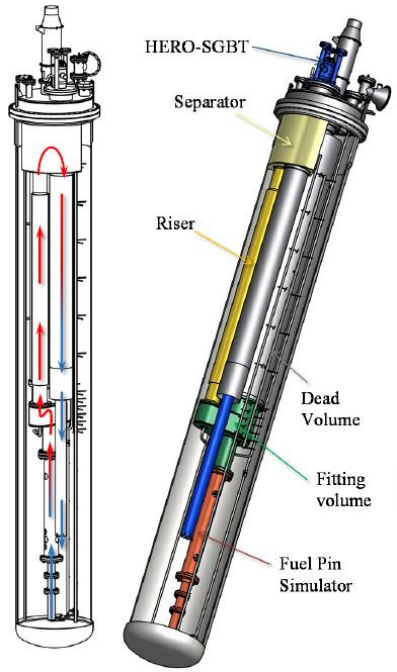

Figure 1: CIRCE-HERO facility (taken from Pesetti et al., 2018)

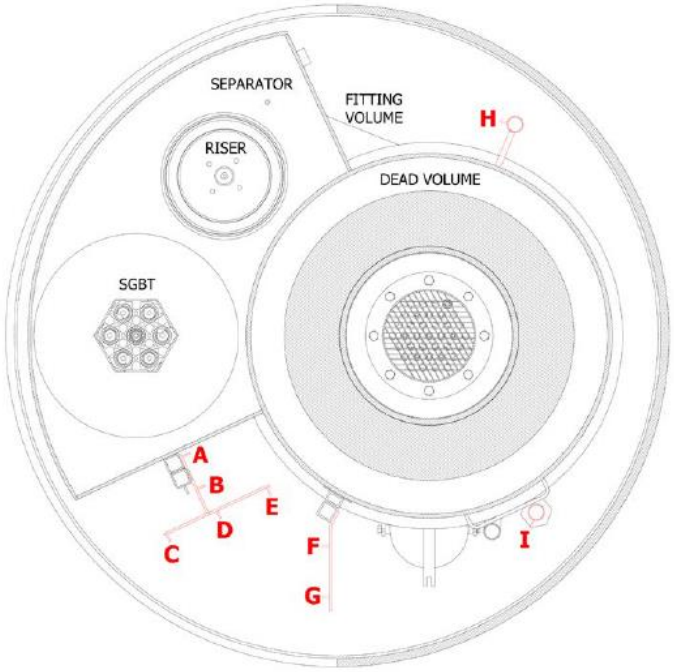

Figure 2: Radial section of the CIRCE facility and thermocouples positions (taken from Pesetti et al., 2018)

Pre Print

3. Adopted mesh and numerical modelling

The main purpose of this paper is to investigate the temperature stratification in the CIRCE-HERO pool. A three-dimensional CFD domain was generated reproducing the CIRCE pool thus excluding the internal HERO loop. In fact, as Figure 3 shows, the internal components are not part of the CFD domain and thus require suitable choices for the boundary conditions to be imposed.

In particular, according to the selected CFD domain, a mass flow rate was imposed at the HERO outlet section (which represents the pool inlet section), while a static pressure was imposed at the FPS inlet section, which represents instead the pool outlet section, see e.g. Figure 4. Regarding the thermal boundary conditions on the pool external walls, a convective boundary condition was imposed for all the simulations. In accordance with previous works (Pucciarelli et al., 2019), a room temperature of 298.15 K together with an external heat transfer coefficient of 2.5 W/(m^{2}K) were chosen, taking into account the thermal resistance of the thermal insulation and external air. On the FPS, the fitting volume and the separator walls, either imposed temperature or convective conditions were considered. Particularly, along the FPS active length, a linear temperature trend that simulates the assumed bulk temperature trend inside the FPS was considered for all the calculations. A constant temperature was instead assumed for both the Fitting Volume and the

Separator. The temperature values were imposed in agreement with the experimental values which were measured inside the HERO loop components. All the other surfaces were considered adiabatic.

Regarding the pool inlet section (HERO-SGBT outlet) a sensitivity analysis accounting for the effects of its shape was also performed. Two different geometrical shapes were considered and reported in Figure 4. This analysis was performed in order to assess the impact on CFD predictions of some simplifying assumptions that may be considered for the HERO outlet section, since it consists in both flow section abrupt changes and interactions with spacer grids, thus implying a high complexity degree. As a consequence, a simpler circular geometry of the size of the HERO external shroud and a hexagonal shape, also accounting for the seven circular bayonet tubes are taken into account.

As previously mentioned, the STAR-CCM+ and the ANSYS Fluent CFD codes were used for the analysis; the meshes were generated adopting the native meshing tools for both the applications. In STAR-CCM+ a polyhedral mesh was generated, while a tetrahedral mesh was adopted for the ANSYS Fluent environment. The most relevant characteristics of the meshes are reported in Table 2. Figure 3a reports a plane section of the STAR-CCM+ mesh, Figure 3b reports instead a detail showing the adopted near wall refinement; Figure 3c and Figure 3d show instead the nodalization created for ANSYS Fluent. RANS calculations were performed adopting three distinct turbulence models: the SST k-ω (Menter, 1994), AKN (Abe et al., 1994) and Standard Lien k-ε (Lien et al., 1996). To improve simulations quality a second-order numerical scheme for all the equations was used and the "All y^+ Wall Treatment" was adopted.

Mesh validation was performed using a refined mesh with a base size of 0.01 m, counting about 10 million cells. As reported in the next section, only negligible differences occur between the calculated temperature trends provided by the refined mesh and the ones described in Table *2*. The coarser meshes were consequently adopted.

	Base size [m]	Number of prism layers	Prism layer stretching	Prism layer thickness [m]	Total number of cells
STAR-CCM+	0.03	5	1.5	0.01	$2.8 \cdot 10^6$
Fluent	0.03	5	1.5	0.01	$2.9 \cdot 10^6$

Table 2: Fluent and STAR-CCM+ mesh settings

Pre Print

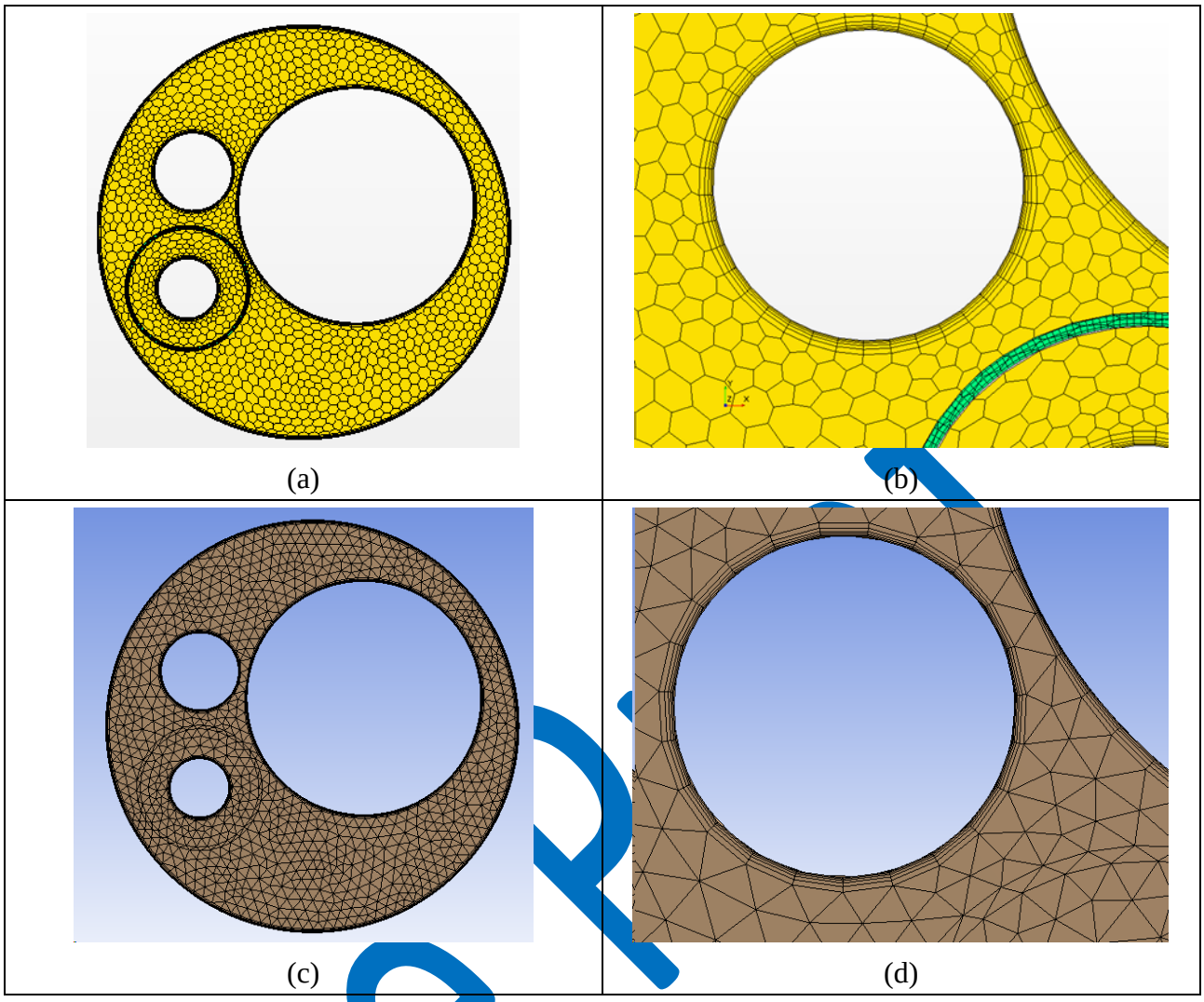

Figure 3: Radial section of the mesh and corresponding magnification obtained with STAR-CCM+ (a) and (b) and ANSYS Fluent (c) and (d) respectively

Pre

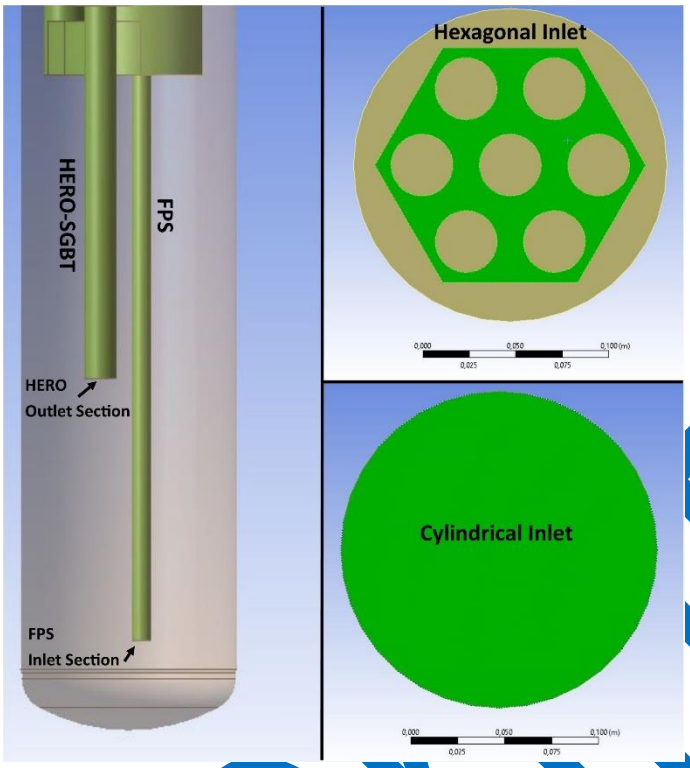

Figure 4: Pool inlet and outlet sections (left) and considered inlet section configurations (right)

Pre Print

4. Obtained results

4.1 Sensitivity analysis

In this section, results obtained with the STAR-CCM+ (Siemens, 2019) code using the simpler cylindrical HERO outlet section are reported. In particular, the Reference Test (see Table 1) is considered for the first analyses, aiming at understanding the effect of adopting different turbulence models or boundary conditions. Figure 5 shows the top view of the considered CFD domain; in particular, the four highlighted positions are selected as probes for the sake of comparison of the measured and calculated trends. It is worth underlining that the position labelled as "S" is in the region where most of the thermocouples are allocated (see Figure 2). Figure 6 reports the comparison of the calculated axial temperature trends and the experimental data for the reference test in case an imposed temperature is assumed for the internal walls; the vertical positions are reported assuming the bottom of the separator as the reference height. Comparing computational results with experimental ones, it can be easily noted that negligible differences occur for the four temperature axial distributions (N, W, E and S), thus suggesting that the thermal distribution mainly depends on the relative height, while the azimuthal position has only a limited influence. Therefore, in the next figures only calculated results relative to the "S" position are reported. Figure 7 shows the results of the sensitivity analysis aiming at understanding the influence of the selected turbulence model: SST k-ω, AKN and Standard-Lien k-ε are considered. As it can be noted, no significant differences occur; the SST k- ω model is consequently selected in the subsequent calculations, since it provides in general more stable numerical resolution processes. The results of a sensitivity analysis investigating the effect of different thermal boundary conditions is instead reported in Figure *8*. Convective conditions with three distinct heat transfer coefficient values were tested and compared with the experimental data. The results show that a good comparison is achieved when adopting a heat transfer coefficient of 5000 W/(m^{2}K) that can be considered a reasonable value for the convective heat transfer coefficient for the fluid flowing inside the loop test section. As a consequence, this boundary condition was selected for all the following calculations.

Pre Print

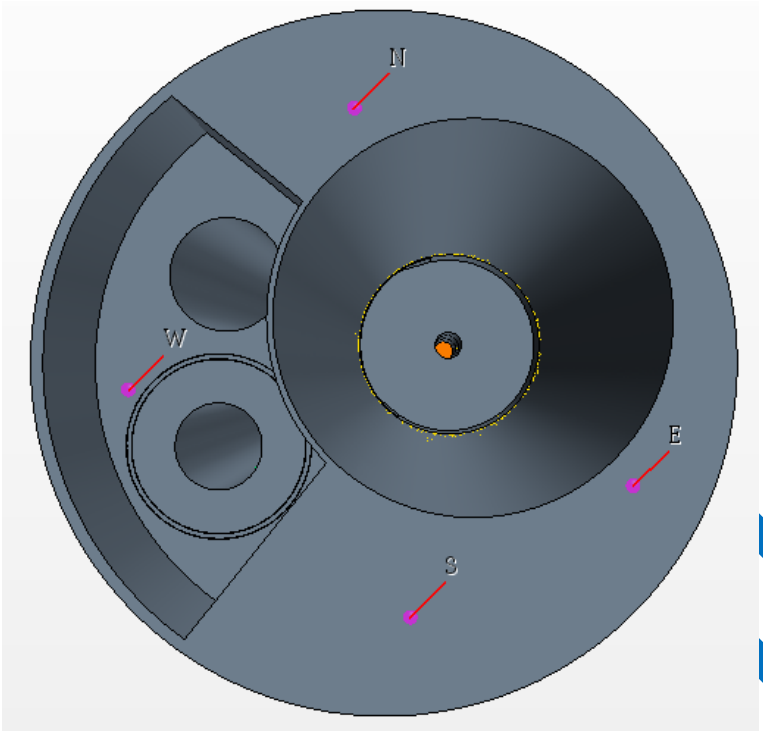

Figure 5: Azimuthal axial temperature positions

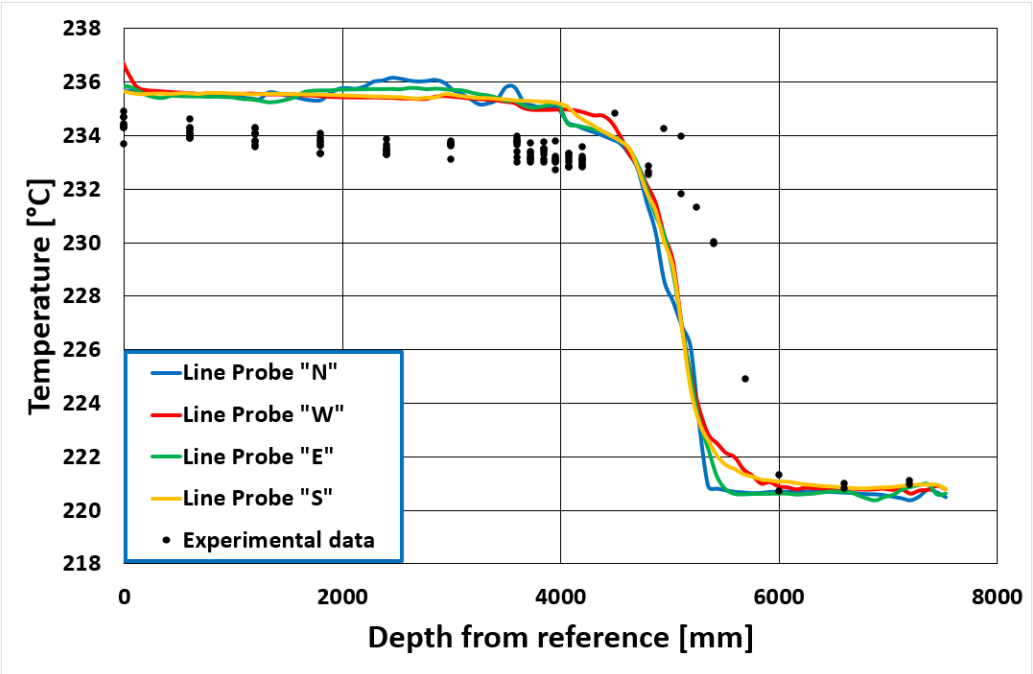

Figure 6: CFD azimuthal positions comparison

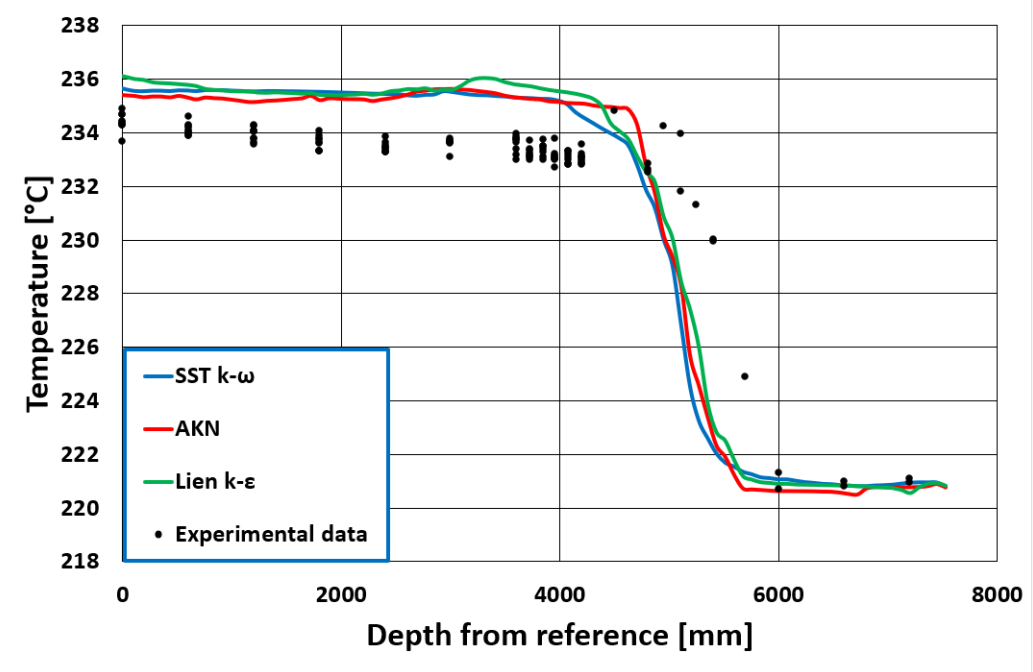

Figure 7: Comparison of the results obtained with 3 different turbulence models STAR-CCM+

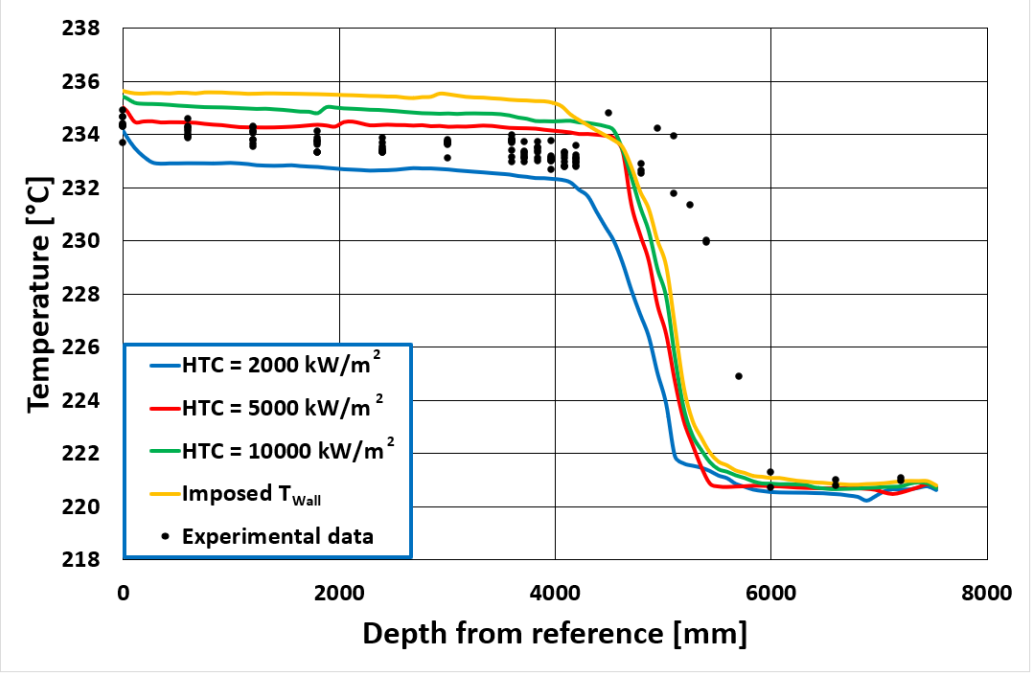

Figure 8: Comparison of the results obtained with 4 different boundary conditions (STAR-CCM+)

4.2 Tests analysis

In this paragraph, numerical results obtained using STAR-CCM+ and ANSYS Fluent codes for the selected steady-states are compared with the experimental results. All the simulations were performed using the SST k-ω turbulence model and the convective thermal boundary condition; a convective heat transfer coefficient of 5000 W/m^{2}K for the heating walls of the FPS, Fitting Volume and Separator is imposed in all the calculations. As anticipated in the previous paragraph, two

different geometries were tested for the inlet section. Figure *9* shows the results obtained for the reference test. As it can be noted, there are no significant differences between the predictions provided by Fluent and STAR-CCM+; some discrepancies instead appear when the two distinct inlet geometries are considered. In particular, adopting the hexagonal configuration, the region in which temperature sharply increases moves upwards (i.e. left in the referred Figure), resulting in a larger discrepancy with the experimental trend. The calculation obtained adopting the refined mesh is reported as well, the observed discrepancies are negligible, thus confirming that the coarser mesh, always adopted in the present work, is sufficiently refined for granting mesh convergence. Figure *10* reports the temperature distribution inside the CIRCE pool for a selected longitudinal section: results obtained for both the considered inlet geometry configurations and codes are shown. It can be observed that, using the hexagonal configuration (Figure *10*a and Figure *10*c), the temperature increase occurs about 0.5 m above the location at which it instead occurs when adopting the cylindrical shape (Figure *10*b and Figure *10*d). This result probably has a fluid-dynamic explanation: in fact, since the hexagon shape implies a smaller flow section, maintaining the imposed mass flow rate it generates a higher average velocity at the inlet section. As a consequence, the fluid dynamics of the pool changes abruptly. As Figure *11* clearly shows, the hexagon configuration implies a larger recirculation zone of "cold" fluid coming from the HERO SGBT. In fact, with this configuration, the cold fluid entering into the pool from the HERO-SGBT hits the bottom of the pool and maintains sufficient momentum for penetrating the hot layer and reaching a region well above the inlet section. Conversely, the cylindrical inlet section, implying a lower inlet velocity, reduces the extension of the recirculation region. Due to the excellent conductive capabilities of liquid metals, the temperature field is strongly connected with the velocity field, thus the region affected by the recirculation phenomena generally coincides with the lower temperature region. This can be clearly observed comparing the temperature fields in Figure *10*c and Figure *10*d with the pathlines reported in Figure *11*. In general, the numerical prediction reproduces sufficiently well the experimental data; the temperature increase occurs in correspondence of the FPS active length below the fitting volume, which is coherent with the imposed boundary conditions. In particular, the total thermal power transferred to the pool by the loop components is about 14 kW and it is distributed as follows: 50% associated to the fitting volume, 40% associated to the FPS and only 10% related to the separator. This value is consistent with the experimental data. Using an energy balance for the reference test, in fact about 13 kW of thermal power are estimated being transferred from the internals to the pool and from the pool to the external environment (Lorusso et al., 2018). As a general comment, the performed calculations suggest that the pool may be considered as a thermal sink at a given temperature close to the one of the fluid flowing inside the fitting volume. The pool is cooled by the flow exiting the HERO-SGBT component; the thermal stratification is defined by the region directly influenced by the entering flow.

Pre Print

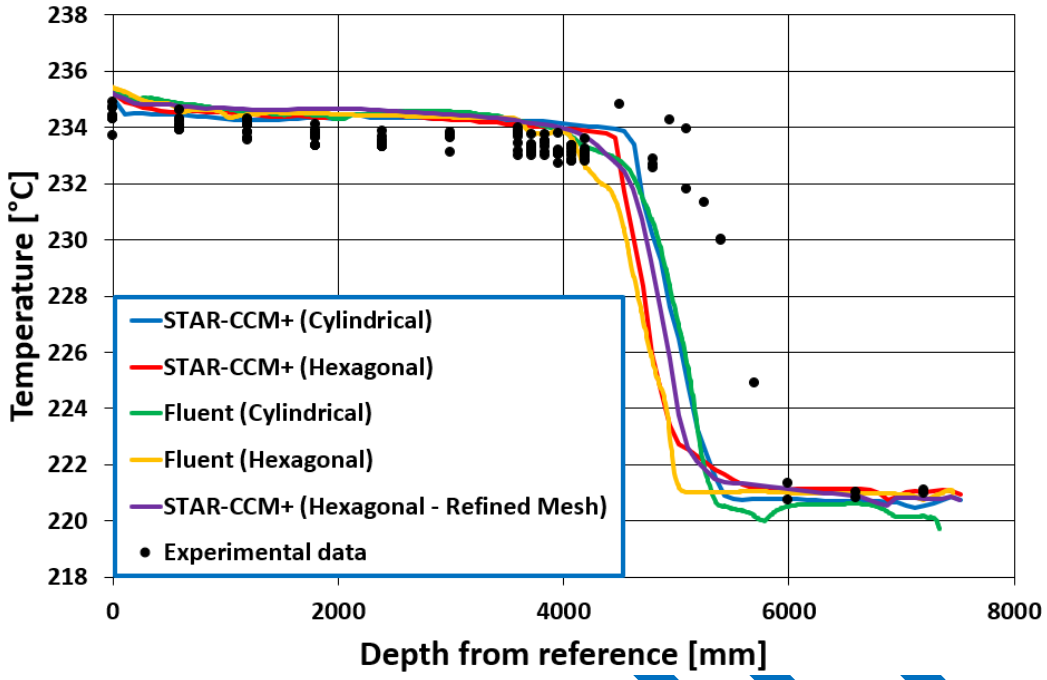

Figure 9: Calculated and experimental axial temperature trends for Test Reference

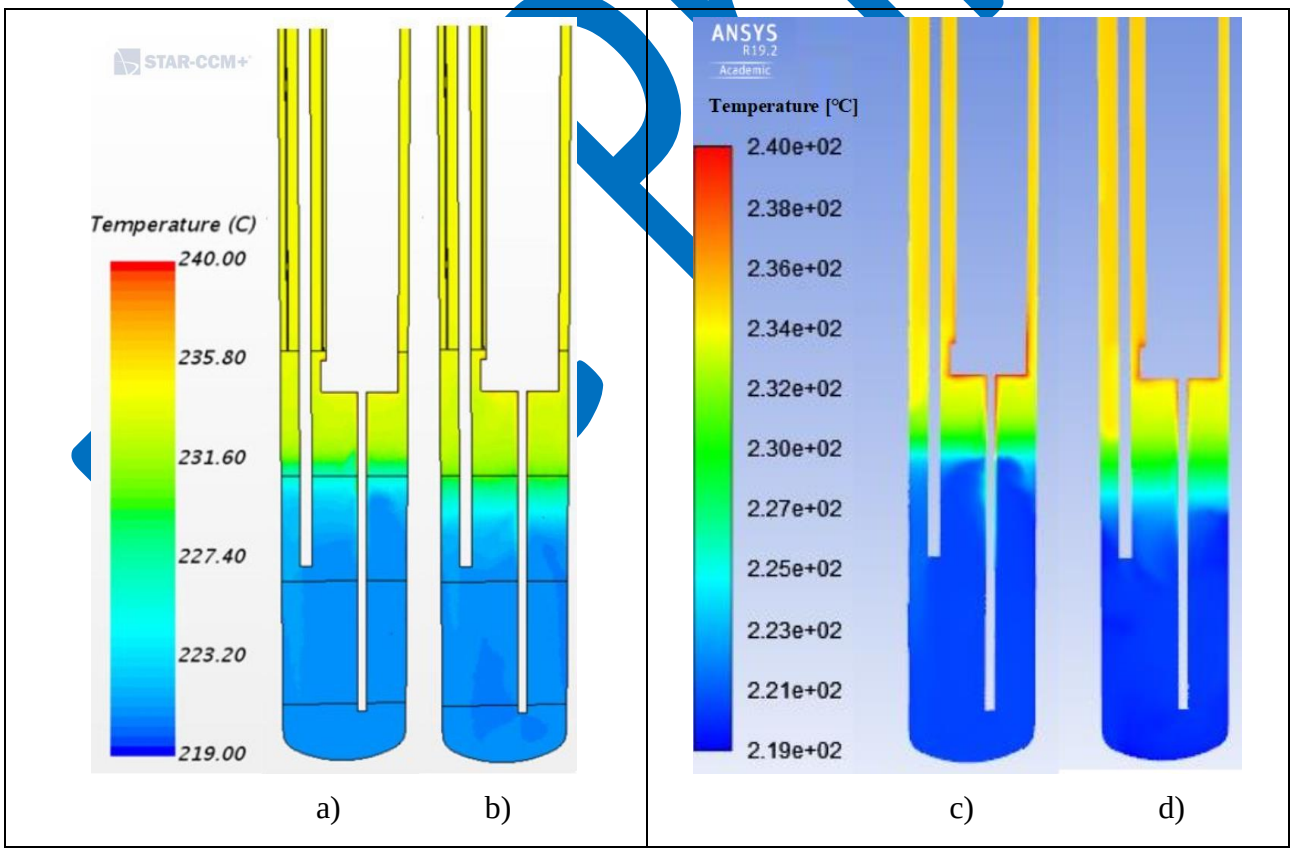

Figure 10: Temperature stratifications: a) STAR-CCM+ (hexagon-inlet), b) STAR-CCM (cylindrical inlet), c) Fluent (hexagon-inlet), d) Fluent (cylindrical-inlet)

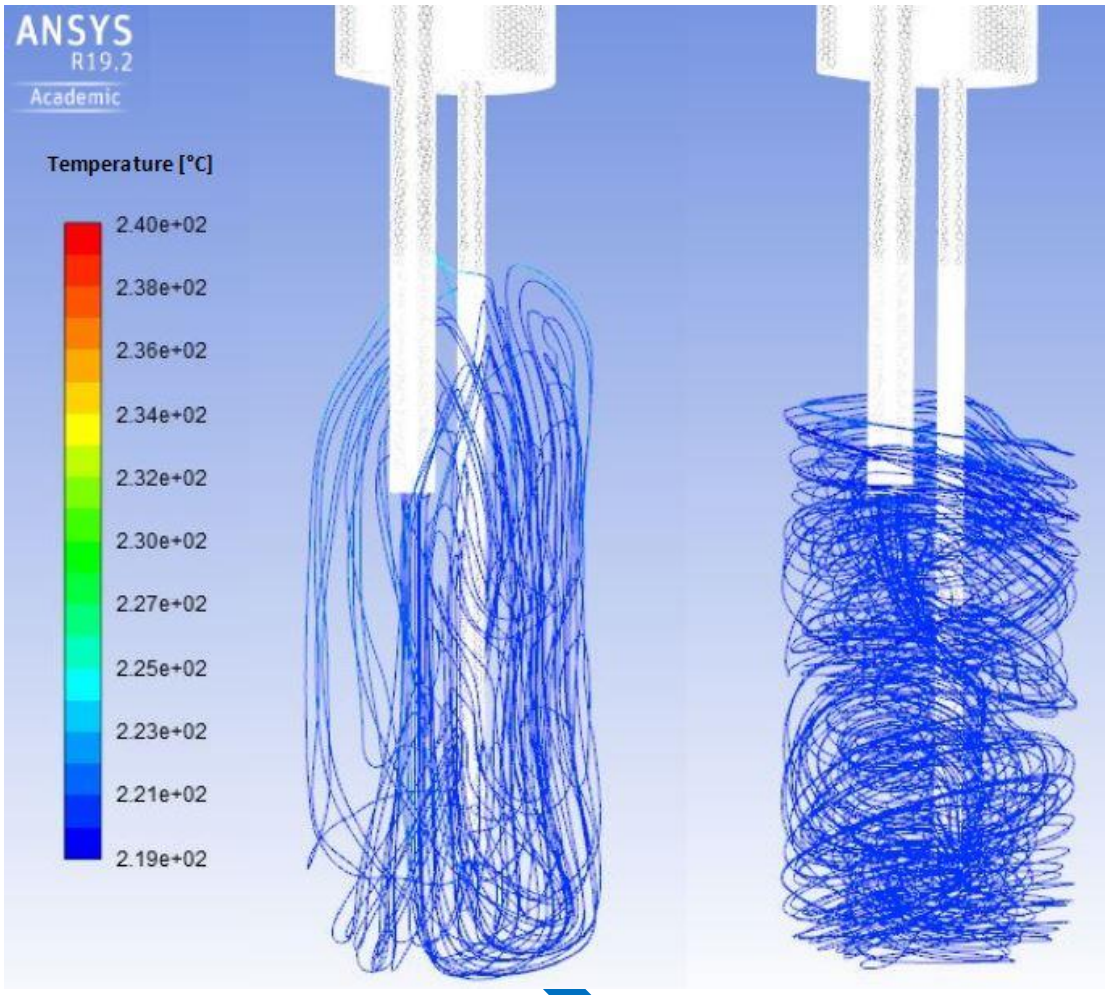

Figure 11: Pathlines for a) Fluent (hexagon-inlet) and b) Fluent (cylindrical-inlet)

Pre-

In Figure 12 the comparison between experimental results and CFD calculations obtained for Test 1 are reported: the obtained results suitably reproduce the measured data. The power supplied in the FPS (140 kW) is significantly larger than the one supplied in the reference test (90 kW); nevertheless, the two stratification trends are very similar, the temperature increase in facts roughly occurs at the same depth. This is a consequence of the imposed inlet mass flow rate. As observed for the reference test in fact (see Figure 12), the predicted temperature stratification trends strongly depend on the inlet velocity distribution. Since the two cases share a very similar mass flow rate, a qualitatively similar stratification trend (in terms of temperature increase region positioning) is to be expected; nevertheless, in accordance with the higher supplied power, higher temperatures are predicted for Test 1.

Figure 13 shows the comparison between the predicted results and experimental data for Test 2. In this case it can be noted that, coherently with the lower supplied power at the FPS comparing to other selected cases, very small temperature increases were experimentally observed inside the pool. Owing to these small discrepancies, it is quite difficult for the codes to exactly reproduce the thermal stratification phenomena; nevertheless, it can be observed that the general temperature

trends were sufficiently well reproduced by CFD calculations even in this case. The upward shift of the transition region, in particular in the case assuming the hexagonal shape for the HERO outlet section, may be connected with predicted too strong effects of the recirculation phenomena, in association with an underestimation of the heat transfer conditions on the FPS external walls. Together with the cited small temperature gradients, this may also due to the intrinsic limits of the adopted CFD tools in predicting heat transfer in such low-turbulence conditions. Taking into account the challenging conditions and the considered assumptions regarding the pool geometry, the obtained results are considered acceptable.

Figure 14 reports the numerical and experimental results relative to Test 3. In this case, the thermal boundary conditions are comparable to the ones of the reference test; the imposed mass flow rate is instead significantly larger (from 30 to 39 kg/s). As a consequence, the obtained temperature values are quite similar; nevertheless, in the CFD results, the temperature transition region slightly shifts upwards. This seems coherent with the imposed higher inlet velocity, which induces a broader recirculation region at the bottom of the pool. As a result, a thicker cold region is coherently predicted. On the other hand, a similar phenomenon seems less relevant in the experimental measurements, in which changes of the imposed mass flow rate only have a limited impact on the positioning of the temperature increase region. This fact may be due to intrinsic underestimations of the pool side convective heat transfer coefficient provided by CFD codes, resulting in a larger impact of the fluid dynamic boundary conditions on the obtained results. Nevertheless, as observed for the other tests, CFD and experimental results show sufficiently similar temperature stratifications trends; temperature is underestimated in the upper part of the pool, but the investigated phenomenon is in general successfully reproduced.

Print

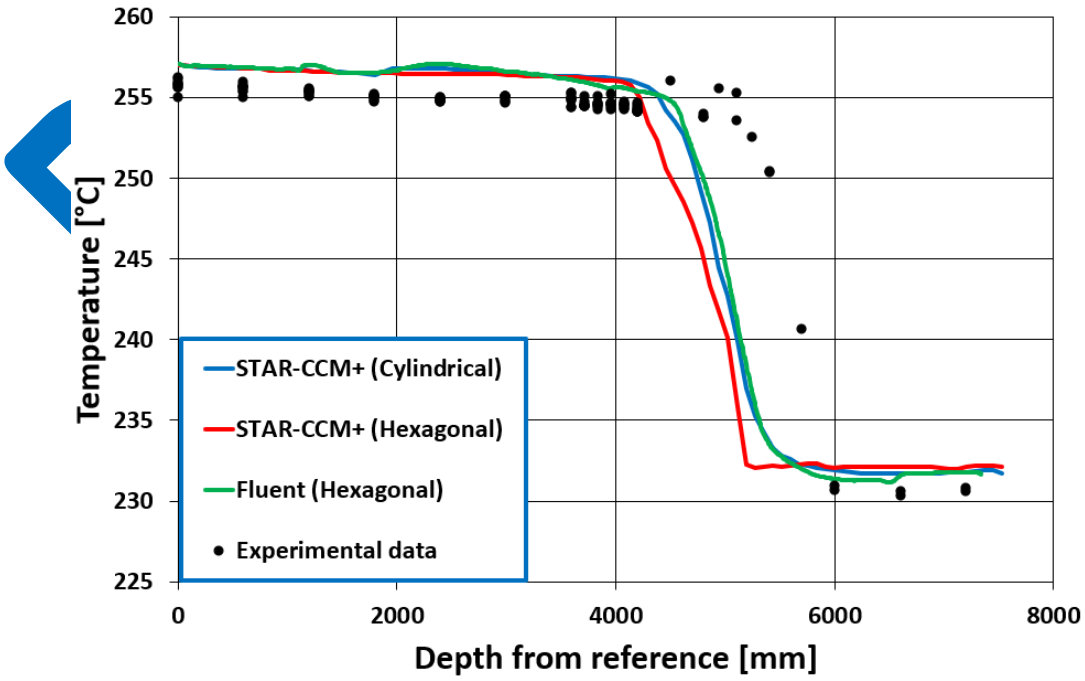

Figure 12: Calculated and experimental axial temperature trends for Test 1

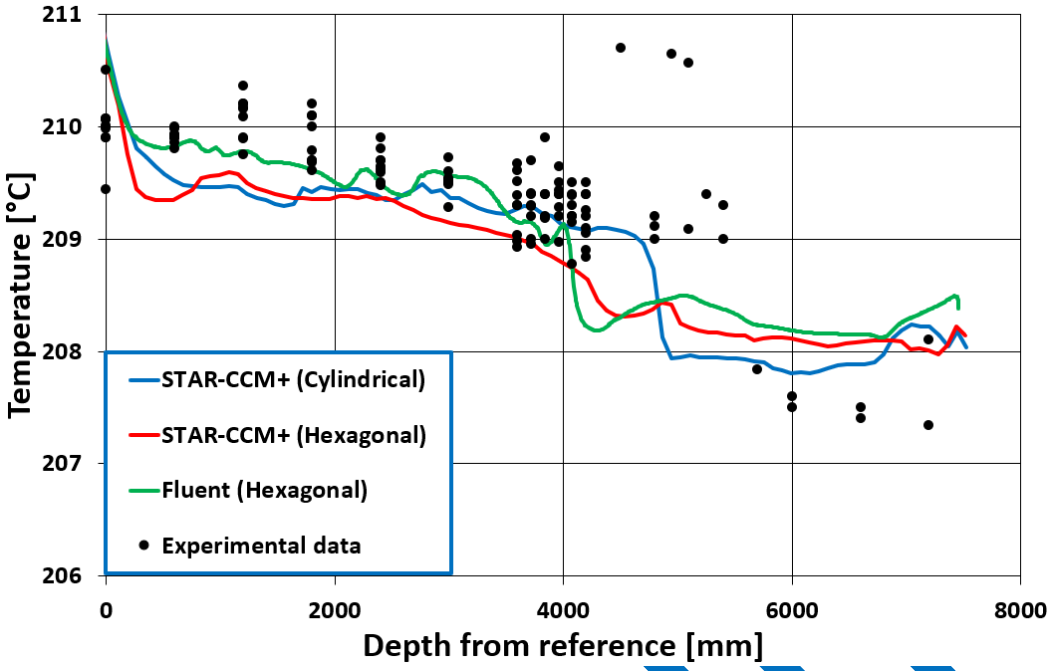

Figure 13: Calculated and experimental axial temperature trends for Test 2

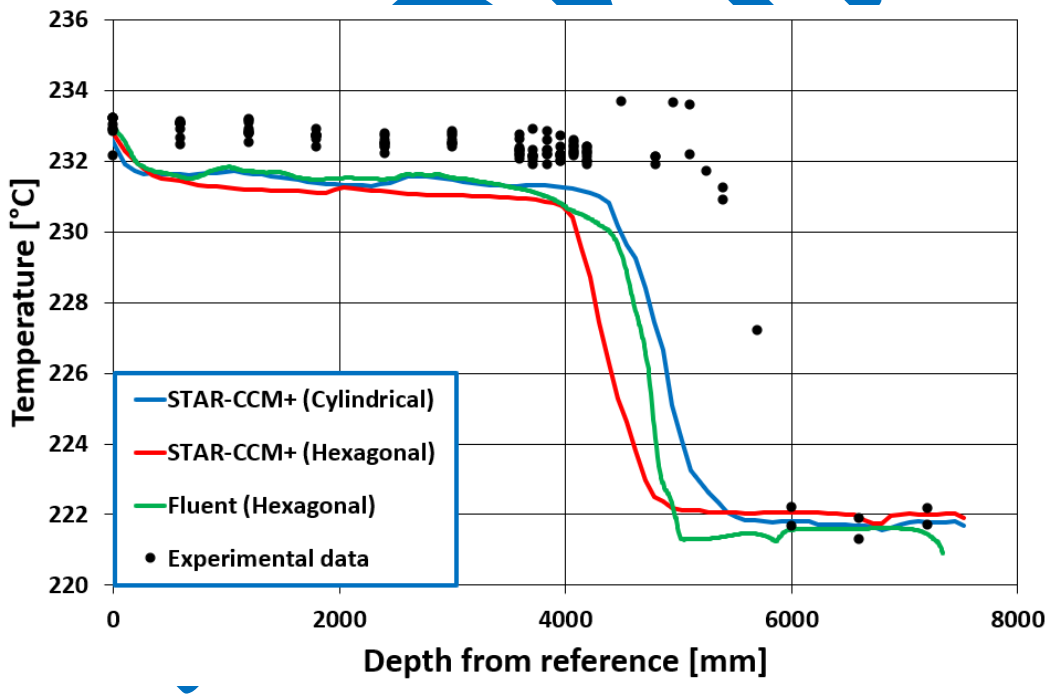

Figure 14: Calculated and experimental axial temperature trends for Test 3

5. Conclusions

In the present paper CFD analyses investigating the temperature stratification phenomena observed in the CIRCE-HERO experimental facility were performed.

In particular, the thermal-hydraulic phenomena occurring in the pool were considered, taking into account both the heat transfer from the internal components to the pool and from the pool to the external environment. Sensitivity analyses regarding both the imposed boundary conditions and the inlet test section geometry were performed highlighting interesting consequences on the predicted trends.

The analysis of the influence of the inlet section configuration clearly showed the impact of the velocity distribution on the obtained CFD thermal stratification trend. Higher velocities in fact imply thicker cold layers, which are associated with the induced broader recirculation regions. The convective heat transfer conditions imposed on the thermal boundaries proved to be reasonable, providing a suitable prediction of the temperature stratification inside the pool.

As a final comment, the adopted CFD codes proved to be a very useful tool for the assessment of the addressed phenomena. The obtained results reproduce sufficiently well the experimental data and provide interesting material for a better understanding on the thermal hydraulics phenomena leading to the observed thermal stratification.

The outcomes of the present work will be used in the frame of future coupled STH/CFD codes applications, aiming at reproducing the whole CIRCE-HERO facility. In fact, as observed in previous studies performed at the University of Pisa, this is a valuable approach for the simulation of long transient involving thermal hydraulics phenomena in complex geometries. The use of a CFD domain simulating the CIRCE pool, in fact, allow a better analysis of 3D pool environment and of the thermal stratification phenomenon, which instead could hardly be captured by the STH code.

Further investigations of the LBE inlet conditions are also envisaged. In particular, structures located in the HERO-SGBT component, slightly upstream the presently considered pool inlet section will be considered in order to assess their influence on the inlet turbulence and velocities distribution, evaluating their impact on the predicted stratification phenomenon. Possible strategies aiming at improving the predicting capabilities of the convective heat transfer conditions will be investigated as well.

Pre Print

Acknowledgments

This work was performed in the framework of H2020 MYRTE project. This project has received funding from Euratom research and training program 2014-2018, under grant agreement No 662186.

6. References

Abe, K., Kondoh, T., and Nagano, Y."A new turbulence model for predicting fluid flow and heat transfer in separating and reattaching flows --- 1. Flow field calculations", Int. J. Heat Mass Transfer, 37, 1994, pp. 139-151.

Angelucci, M., Martelli, D., Barone, G., Di Piazza, I., Forgione, N., "STH-CFD Codes Coupled Calculations Applied to HLM Loop and Pool Systems", Science and Technology of Nuclear Installations, 2017a, Article ID 1936894.

Angelucci, M., Forgione, N., Martelli, D., Tarantino, M., "RELAP5 STH and Fluent CFD coupled calculations of a PLOHS +LOF transient in the HLM experimental facility CIRCE", International Conference on Nuclear Engineering, ICONE 2017, Shanghai, China, 2-7 July 2017, 2017b

ANSYS, Inc., "*ANSYS Fluent User's Guide, Release 19.2*", August 2018.

Di Piazza et al., "Nacie-UP: an heavy liquid metel loop for mixed convection experiments with instrumented pin bundle" HLMC-2013, 2013.

Forgione, N., Angelucci, M., Ulissi, C., Martelli, D., Barone, G., Ciolini, R., Tarantino, M., "Application of RELAP5/Mod3.3 – Fluent coupling codes to CIRCE-HERO", Journal of Physics: Conference Series. IOP Publishing, 2019. p. 012032.

Generation IV International Forum (GIF). "*Technology Roadmap Update for Generation IV Nuclear Energy Systems*", 2014.

Gonfiotti, B., Barone, G., Angelucci, M., Martelli, D., Forgione, N., Del Nevo, A., Tarantino, M., "*Thermal hydraulic analys of the circe-hero pool-type facility*", International Conference on Nuclear Engineering, Proceedings, ICONE Volume 6B, 20182018 26th International Conference on Nuclear Engineering, ICONE 2018; London; United Kingdom; 22 July 2018 through 26 July 2018; Code 141167

Lien, F.S., Chen, W.L., Leschziner, M.A., *"Low-Reynolds number eddy viscosity modelling based on non-linear stress-strain/vorticity relations"*. Proceedings of the 3rd Symposium on Engineering Turbulence Modelling and Measurements, 27-29 May, 1996, Crete, Greece.

Lorusso, P., Pesetti, A., Tarantino, M., Polazzi, G., Sermenghi, V., "CIRCE Experiment report" ENEA report for Project MYRTE, Ref. CI-I-R-353, 2018.

Pre Print

Martelli, D., Forgione, N., Barone, G., Del Nevo, A., Di Piazza, I., Tarantino, M., "*Coupled simulations of natural and forced circulation tests in NACIE facility using relap5 and Ansys fluent codes"* 2014 22nd International Conference on Nuclear Engineering, ICONE 2014; Prague; Czech Republic; 7 July 2014 through 11 July 2014; Code 109131.

Martelli, D., Marinari, R., Barone, G., Di Piazza, I., Tarantino, M., "*CFD thermo-hydraulic analysis of the CIRCE fuel bundle"*, Annals of Nuclear Energy, Volume 103, 1 May 2017, Pages 294-305, 2017a

Martelli, D., Forgione, N., Barone, G., Di Piazza, I., "Coupled simulations of the NACIE facility using RELAP5 and ANSYS FLUENT codes", Annals of Nuclear Energy, Vol. 101, pp. 408-418, 2017b.

Narcisi, V., Giannetti, F., Tarantino, M., Martelli, D., Caruso, G., *"Pool temperature stratification analysis of CIRCE-ICE facility with RELAP5-3D© model and comparison with experimental tests"*, Journal of Physics: Conference Series, Volume 923, Issue 1, 20 November 2017, Article number 01200635th Italian Union of Thermo-Fluid Dynamics Heat Transfer Conference, UIT 2017; Faculty of Engineering, Marche Polytechnic University Ancona; Italy; 26 June 2017 through 28 June 2017; Code 131974

Menter, F.R., "*Two-equation eddy-viscosity turbulence modelling for engineering applications*". AIAA Journal 32(8) pp. 1598-1605, 1994.

Pesetti, A., Forgione, N., Narcisi, V., Lorusso, P., Giannetti, F., Tarantino, M., "ENEA CIRCE-HERO test facility: geometry and instrumentation description", ENEA report for Project H2020 SESAME Project WP5.2, Ref. CI-I-R-343, 2018a.

Pesetti, A., Lorusso, P., Polazzi, G., Sermenghi, V., Tarantino, M., "CIRCE-HERO test facility: heat losses characterization tests", ENEA report, Ref. CI-I-R-351, 2018b.

Pucciarelli, A., Forgione, N., Martelli., D., Dovizio, D., Zwijsen, K., Moreau, V., Lampis, S., "*CIRCE Pos-test CFD calculation report*", Report D3.4 of the MYRTE project, Grant Agreement number: 662186 - Activity: NFRP-09-2015, 2019

Siemens, "*USER GUIDE STAR-CCM+ Version 13.06.011",* 2018.

Tarantino, M., Agostini, P., Benamati, G., Coccoluto, G., Gaggini, P., Labanti, V., Venturi, G., Class, A., Liftin, K., Forgione, N., Moreau, V., "*Integral Circulation Experiment: Thermal-hydraulic simulator of a heavy liquid metal reactor*", Journal of Nuclear Materials 415r, 433-448, 2011

Pre Print